Journal of Vertebrate Paleontology e2080556 (7 pages)

DOI: 10.1080/02724634.2021.2080556

ARTICLE

REAPPRAISAL OF THE LATE MIOCENE ELASMOTHERIINE *PARELASMOTHERIUM SCHANSIENSE* FROM KUTSCHWAN (SHANXI PROVINCE, CHINA) AND ITS PHYLOGENETIC RELATIONSHIPS

PANAGIOTIS KAMPOURIDIS, [1,*] JOSEPHINA HARTUNG, [1] GABRIEL S. FERREIRA, [1,2] and MADELAINE BÖHME[1,2]
[1]Eberhard Karls University of Tübingen, Tübingen 72076, Germany, pkampouridis94@gmail.com;
[2]Senckenberg Centre for Human Evolution and Palaeoenvironment, Tübingen 72076, Germany

ABSTRACT—Elasmotheres, such as the huge Siberian unicorn (*Elasmotherium sibiricum*), are amongst the most iconic large mammals ever to roam Eurasia. Several different elasmotheriine taxa are also known from the upper Miocene of Asia, including the large genus *Parelasmotherium*. Herein we present the re-examination of the holotype of its type species *Parelasmotherium schansiense*, using high resolution X-ray computed tomography. The μCT analysis reveals thus far unknown morphological features of the M1 and the unerupted P4 and M2, thereby adding to our knowledge about this species. This allows comparisons with other species that have been referred to *Parelasmotherium*, '*Parelasmotherium*' *simplum* and '*Parelasmotherium*' *linxiaense*, which, according to the results of the phylogenetic analysis, should not be included in the same genus as *P. schansiense*. Furthermore, based on comparisons to other Miocene elasmotheriines the diagnosis of *Parelasmotherium schansiense* was amended and its phylogenetic position was assessed. *Parelasmotherium schansiense* is placed in a monophyletic group of 'derived elasmotheriines,' which also includes the genera *Elasmotherium*, *Sinotherium*, and *Ninxiatherium*.

SUPPLEMENTAL DATA—Supplemental materials are available for this article for free at www.tandfonline.com/UJVP.

Citation for this article: Kampouridis, P., J. Hartung, G. S. Ferreira, and M. Böhme. 2022. Reappraisal of the late Miocene elasmotheriine *Parelasmotherium schansiense* from Kutschwan (Shanxi Province, China) and its phylogenetic relationships. Journal of Vertebrate Paleontology. DOI: 10.1080/02724634.2021.2080556

INTRODUCTION

Elasmotheres are amongst the most characteristic rhinocerotids found in the fossil record. This group of rhinos existed throughout the Old World (e.g., Antoine, 2002; Geraads et al., 2012; Deng et al., 2013), but prevailed in Asia, where it survived until the latest Pleistocene (Kosintsev et al., 2019; Liu et al., 2021). The affinities and relationships of its representatives remained enigmatic for a long time, but during the last decades numerous new finds have elucidated the evolutionary history of this unique group (Antoine, 2002; Schvyreva, 2015; Kosintsev et al., 2019). However, the taxonomy and phylogeny of its pre-Quaternary representatives are not fully resolved (e.g., Fortelius and Heissig, 1989; Geraads et al., 2012; Deng et al., 2013). The aim of this study is to re-describe the holotype of the huge *Parelasmotherium schansiense* Killgus, 1923 (Fig. 1), a late Miocene representative of elasmotheriines. High resolution X-ray computed tomography was used to reveal previously unknown information about the internal tooth morphology of its holotype; thus, allowing for detailed comparisons to the other elasmotheriines, elucidating their phylogenetic relationships, especially within the genus *Parelasmotherium*.

LOCALITY

Parelasmotherium schansiense was originally described by Killgus (1923), based on material from the upper Miocene locality of Kutschwan, Shanxi Province, China. The material was excavated by Albert Tafel from sediments on the Chinese Loess Plateau along the Yellow River in 1905 (Tafel, 1914; Killgus, 1922, 1923), over a decade before the first excavation of Johan Gunnar Andersson in Shanxi (Andersson, 1923). The material was later given to the Eberhard Karls University of Tübingen (Germany), where it was studied by Hugo Killgus for his Ph.D. dissertation (Killgus, 1922). Unfortunately, the exact geographical location of Kutschwan remains unknown. The fossils of Kutschwan represent a typical large mammal assemblage of the upper Miocene of China. They include the hornless rhino *Chilotherium habereri*, *Hipparion* sensu lato, the large giraffid *Schansitherium tafeli*, two bovids, and an ictithere hyaenid, along with the huge rhino *P. schansiense* (Killgus, 1922, 1923). Adhering particles of red fine silt on the fossils reveal that the embedding sediment represents the classical 'Chinese Red Clay.'

MATERIAL AND METHODS

The holotype of *P. schansiense* consists of four upper teeth (GPIT-PV-86051; Fig. 1) housed in the Geological and Paleontological Institute at the University of Tübingen, Germany (GPIT). To study the internal tooth morphology in detail, micro-computed tomography (μCT) scans were acquired with a Nikon XTH 320 μCT scanner operated by the Centre for Visualisation, Digitisation and Replication at the Eberhard Karls University Tübingen and Senckenberg Centre for Human Evolution and Palaeoenvironment Germany (SHEP). An X-ray tube containing a multi metal reflection target with a maximum acceleration voltage of 225 kV was used. The articulated D4, P4, and M1 were

*Corresponding author
Color versions of one or more of the figures in the article can be found online at www.tandfonline.com/ujvp.

Published online 05 Jul 2022

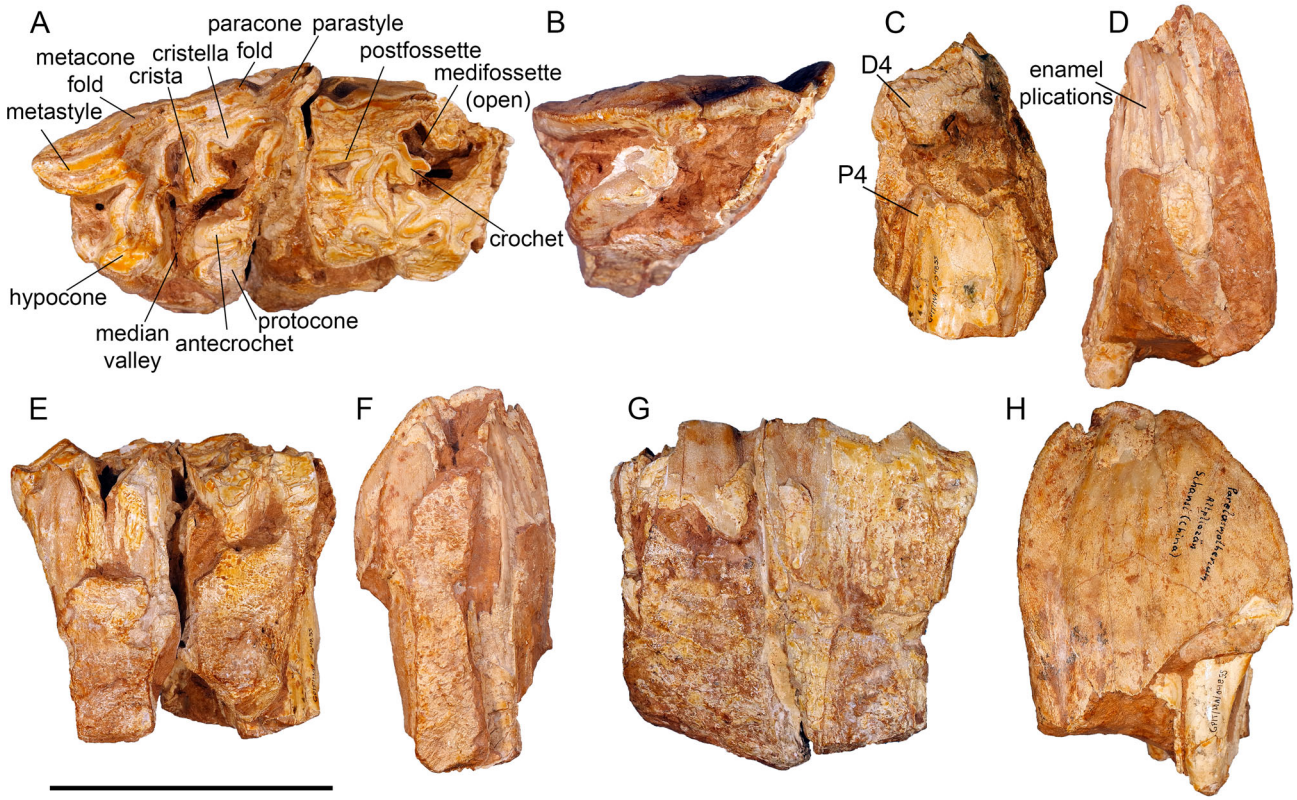

FIGURE 1. Photographs of the holotype of *Parelasmotherium schansiense* (GPIT-PV-86051) from the upper Miocene of Kutschwan (Shanxi Province, China). **A**, **C**, **E**, **G**, articulated right D4 and M1; and **B**, **D**, **F**, **H**, right M2 in occlusal (**A** and **B**), anterior (**C** and **D**), lingual (**E** and **F**), and buccal (**G** and **H**) view, respectively. Note that in posterior view (**C**), both the D4 and P4 are exposed. Scale bar equals 7.5 cm for **A-B** and 10 cm for **C-H**.

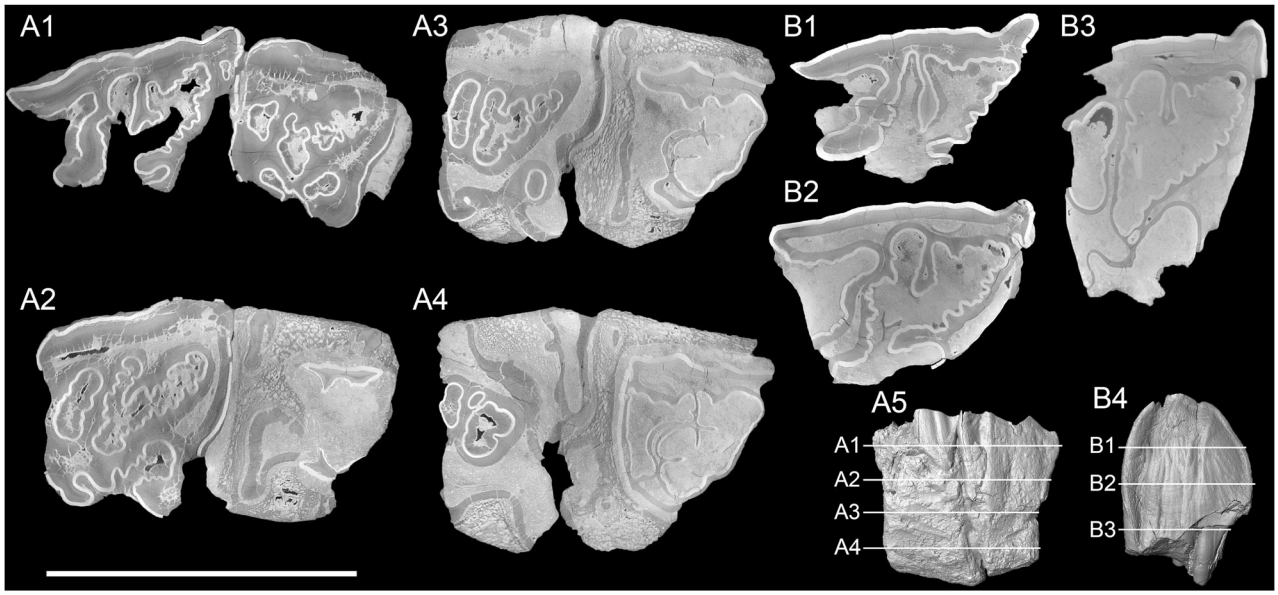

FIGURE 2. µCT-scan orthoslices of the holotype of *Parelasmotherium schansiense* (GPIT-PV-86051) from the upper Miocene of Kutschwan (Shanxi Province, China). **A**, articulated right M1 and D4 (**A1**) or P4 (**A2-4**), in occlusal (**A1–4**) and buccal (**A5**) view; **B**, isolated right M2, in occlusal (**B1-3**) and buccal (**B4**) view. The virtual orthoslices are taken at different positions, as shown in **A5** and **B4**, respectively. Scale bar equals 10 cm for **A1–4** and **B1-3** and 20 cm for **A5** and **B4**.

scanned at 220 kV and 140 μA with a voxel size of 0.05932821 mm, using a copper filter of 0.5 mm thickness. The isolated M2 was scanned at 220 kV and 190 μA with a voxel size of 0.05002721 mm, with the same copper filter. Images were processed using VG Studio Max. The results are virtual orthoslices of the actual teeth (Fig. 2). The scans are available on MorphoSource under the following IDs:

Media ID—000415992 (D4, P4, and M1) and 000416854 (M2).

The dental terminology used in this study is shown in Fig. 1A, D and follows Guérin (1980) and Antoine (2002). Measurements of the teeth are given in Table 1.

SYSTEMATIC PALEONTOLOGY

Class MAMMALIA Linnaeus, 1758
Family RHINOCEROTIDAE Gray, 1821
Tribe ELASMOTHERIINI Dollo, 1885
PARELASMOTHERIUM Killgus, 1923

Diagnosis—Same as for the type species.

Type Species—*Parelasmotherium schansiense* Killgus, 1923.

Remarks—Three further species have been previously attributed to *Parelasmotherium*: *Sinotherium simplum* Chow, 1958, *Parelasmotherium linxiaense* Deng, 2001, and *Ninxiatherium longirhinus* Chen, 1977 (Qiu and Xie, 1998; Deng, 2001; Antoine, 2002). The first two are herein regarded as not belonging to this genus and will provisionally be referred to as '*Parelasmotherium*.' The third species was considered a junior synonym of *P. schansiense*, but was later re-established as a valid taxon, belonging to *Ninxiatherium*, along with *Ninxiatherium euryrhinus* Deng, 2008, which is also supported in this study.

PARELASMOTHERIUM SCHANSIENSE Killgus, 1923 (Figs. 1–2)

Holotype—Partial right upper toothrow, with worn D4 and M1, and unerupted P4 and M2 (GPIT-PV-86051).

Type Locality—Kutschwan, Shanxi Province, China (Baodean; late Miocene).

Amended Diagnosis—Large elasmotheriine with a unique combination of dental features separating it from all other elasmotheriines: large crochets on D4 and P4; well-established protocone and hypocone connection at any wear stage, unconstricted hypocone, presence of a 'pseudometaloph,' and prominent metacone and paracone folds on P4; strongly constricted hypocone and highly plicated enamel in the hypsodont M1 and M2.

Description

D4—This tooth represents the only deciduous tooth preserved. The anterior half of the ectoloph is broken off and the lingual part of the D4 is heavily damaged (Fig. 1A, G). The tooth is moderately worn, and its preserved maximal height is 41 mm. The protocone is very strongly constricted, anteriorly and posteriorly, resulting in a large antecrochet. A large plication is present at the buccal side of the antecrochet. The hypocone is strongly constricted anteriorly, forming a large enamel fold that connects to the antecrochet (Fig. 2A1) with advanced wear, closing the median valley. A small crista is present. A large crochet exists, which splits into two small enamel folds. The lingual one fuses with the enamel plication of the antecrochet, when slightly more worn (Fig. 2A1). The postfossette is closed. On the ectoloph, two folds at the level of the metacone are present and the beginning of a paracone fold can be traced. The tooth is partially filled with cement and some remnants cover part of the ectoloph.

P4—It is not yet erupted. In fact, it is not even fully formed yet, remaining beneath the D4 that is still in use (Fig. 1C). The μCT analysis reveals the previously unknown morphology of the thus far formed P4 (Fig. 2A2–3). The anterior enamel wall of this tooth is completely lacking, due to damage; thus, its morphology cannot be assessed. The P4 exhibits a protocone and hypocone, which are fused right from the beginning. A large double crochet is present that connects to the long but thin crista very early in occlusion. A cristella and a postcrista are present as short enamel bumps. The postfossette closes posteriorly at a very early wear stage, but remains anteriorly connected to the medifossette at all levels of the thus far formed tooth. The hypocone does not connect to the metacone at any level of the formed P4, while the crochet and the crista form a 'pseudometaloph' (sensu Antoine, 2002). Buccally, well-developed metacone and paracone folds are present. The enamel within the tooth exhibits some small enamel bumps, much less distributed than the enamel plications in the two molars.

M1—The M1 is the best-preserved tooth, only lacking the lingual half of the anterior wall and part of the protocone (Fig. 1A, E). It is moderately worn. The protocone bears a very strong posterior constriction, forming a large, lingually-oriented antecrochet. The anterior part of the protocone is damaged, but a small curve in the enamel at the middle of the tooth (Fig. 2A2) confirms the occurrence of an anterior protocone constriction. The hypocone bends posteriorly and bears a strong anterior constriction and a very small posterior constriction on its lingual tip. The protocone and the hypocone fuse when moderately worn. A large crista is present, with a strong anteriorly oriented plication. Though, when heavily worn the crista would become less distinct (see Fig. 2A3). Anterior to the crista, a distinct, but weak cristella is present, which connects to the anterior plication of the crista when slightly more worn. A very small crochet is visible that does not connect with the crista. A weak anterior cingulum is present. A posterior cingulum exists, leading to the closure of the postfossette. The ectoloph is relatively flat, albeit exhibiting a prominent paracone fold and a strong parastyle. The M1 has strong internal enamel plications, which are already visible on the posterior enamel wall of the protoloph of the only little worn M1 (Fig. 1A), but become much more widespread and prominent with further wear (Fig. 2A1–3). The M1 exhibits extensive cement covering internally and externally, on all sides of the tooth. The surface of the outer enamel layer is quite wavy and rough.

M2—It is the only tooth that is completely isolated and not enclosed in the maxillary bone (Fig. 1B–F). The tooth is completely unworn, but the protocone and the anterior enamel wall are broken off. Only the μCT analysis reveals the morphology of the M2 (Fig. 2B). It exhibits a strongly posteriorly-constricted protocone that forms a large antecrochet. The presence of an anterior constriction cannot be assessed. The hypocone is strongly constricted anteriorly, forming a large enamel fold that fuses with the antecrochet when moderately worn, closing the median valley. The crista is well developed at an early wear stage (Fig. 2B1), but becomes smaller when heavily worn (Fig. 2B3), a

TABLE 1. Dental measurements of the holotype of *Parelasmotherium schansiense* Killgus, 1923 (GPIT-PV-86051) in mm. The measurements were taken with a digital caliper with an error of 0.01 mm and then rounded. Height: the preserved height is given, the D4 and M1 are already significantly worn and M2 is probably not fully formed yet; HI (Hypsodonty Index = Height/Length) is a minimal value, because the height of the teeth is not complete.

Tooth	Height	Length	Width	HI
D4	41	~55	57	-
M1	115	80	~70	1.44
M2	145	85	~70	1.71

feature that is also visible in *Sinotherium lagrelii* Ringström, 1924 (Ringström, 1924:textfigs. 87–88). A small cristella is present throughout the tooth's height. A small crochet is present. An anterior cingulum is present as shown by a small remnant right below the parastyle. A posterior cingulum is present, leading to the closure of the postfossette, when moderately worn. The ectoloph is slightly wavy with a strong parastyle. The enamel within the tooth is very wrinkled, with strong plications being present mostly on the posterior enamel wall of the protoloph (Fig. 2B). The plications would be visible at a very early wear stage, as demonstrated by the high-placed (about 1 cm below the occlusal surface) enamel plications that are visible through the broken protoloph (see Fig. 1D). The M2 exhibits remnants of cement within the median valley, the postfossette, and on the ectoloph. The surface of the outer enamel layer is quite wavy and rough.

Comparison to Other Species of *Parelasmotherium*

The genus *Parelasmotherium* was erected by Killgus (1923) for *P. schansiense*, based on the material studied here (Figs. 1–2). It was originally based on its large dimensions, high hypsodonty, extensive cement covering and low enamel thickness of the teeth (Killgus, 1922, 1923). Later, three species were included in this genus: *N. longirhinus*, '*P.*' *simplum*, and '*P.*' *linxiaense* (Qiu and Xie, 1998; Deng, 2001; Antoine, 2002). The first taxon was later re-established and is herein treated as a valid taxon. The other two were based on isolated teeth (Chow, 1958; Qiu and Xie, 1998; Deng, 2001), but from the latter a complete skull was later reported (Deng, 2007). The morphology of *P. schansiense* is evidently more complex than the other two species. In '*P.*' *simplum*, the crista is rather small, and a small crochet may be present in the molars, while the enamel shows no signs of plications in the molars (Chow, 1958; Qiu and Xie, 1998). These features remain relatively constant throughout the height of the teeth, as demonstrated by the cross section of the M2 figured by Qiu and Xie (1998:pl. 1, figs. 4-5), thus differing from the molars of *P. schansiense* that bear a huge crista, no crochet and are highly plicated.

The differences of *P. schansiense* to '*P.*' *linxiaense* are somewhat more subtle. The P4 morphology resembles that of *P. schansiense* in having a fused protocone and hypocone, an unconstricted hypocone, as well as a long crochet and crista that connect when worn enough (Deng, 2007:fig. 3). However, the hypocone does not fuse with the metacone and the metacone fold is much stronger in *P. schansiense*, in contrast to '*P.*' *linxiaense*. Although, the missing connection between the hypocone and the metacone might represent a somewhat variable feature, as seen in the 'pseudometaloph' (sensu Antoine, 2002) variably occurring in the P3s of *Sinotherium* (Ringström, 1924:figs. 77-80). More importantly, in the molars of '*P.*' *linxiaense* enamel plications are very weak or absent, as seen both in its holotype (IVPP V 12650; Deng, 2001:pl. 1, figs. 1-3), as well as in the skull discovered later at the same locality (HMV 1411; Deng, 2007:fig. 3). In contrast, in *P. schansiense* plications are very prominent and would be visible on both the M1 and M2 after some slight to moderate wear (Fig. 2A1, B1), and are already beginning to show in the little worn M1 (Fig. 1A). Thus, both '*P.*' *simplum* and '*P.*' *linxiaense* differ from *P. schansiense*, as well as from one another.

Comparison to Other Elasmotheriines from the upper Miocene of China

Iranotherium—*Iranotherium morgani* (Mecquenem, 1908), is best known from its type locality Maragheh, from the upper Miocene of Iran (Mecquenem, 1908; Pandolfi, 2016), but two complete skulls have also been recovered from upper Miocene deposits of the Linxia Basin in China (Deng, 2005). The cheek teeth of *I. morgani* are covered and filled with cement (NHMW 2014/0425/001, pers. obs.; Deng, 2005; Pandolfi, 2016), a common feature in elasmotheriines (Geraads et al., 2016; Geraads and Zouhri, 2021). However, *I. morgani* differs from 'derived elasmotheriines' like as *P. schansiense* in having small or absent cristae, no or extremely weak enamel plications, and the hypocone of the M1 and M2 not posteriorly bent as seen in *I. morgani* from Maragheh (NHMW 2014/0425/001, pers. obs. by P.K.) and from the Linxia Basin (see Deng, 2005:fig. 6).

Ninxiatherium—*Ninxiatherium longirhinus*, is based on a complete skull from Ningxia (China). Antoine et al. (2002) synonymized *P. schansiense* and *N. longirhinus*, considering their differences as possible intraspecific variation, whereas Deng (2007) separated the two genera. This was based on some cranial and dental characters, following the discovery of a complete skull of '*P.*' *linxiaense* that was later further supported by Deng (2008). The present study of the *P. schansiense* holotype confirms the existence of significant differences between *Ninxiatherium* and *Parelasmotherium*. In *N. longirhinus* the P4 bears only very small crista and crochet, and the ectoloph seems very flat (Chen, 1977:fig. 1), in contrast to the long crista and crochet of *P. schansiense*, as revealed by the µCT-scan of the specimen from Kutschwan (Fig. 2A2–4). Moreover, in contrast to *P. schansiense*, the molars of *N. longirhinus* bear widely connected protocone and hypocone, a very small crista, and exhibit no distinct parastyle (Chen, 1977:fig. 1).

Deng (2008) erected the new species *N. euryrhinus*, which differs from *N. longirhinus* in having a larger size, wider nasals, and a shallower nasal notch. The P4 of *N. euryrhinus* bears very short crista and crochet compared to *P. schansiense* (Fig. 2A3–4). The molars of *N. euryrhinus* exhibit a small crista, and the cristella, when present, is very small, in contrast to *P. schansiense*.

Both *N. longirhinus* and *N. euryrhinus* exhibit a hypocone, which is not as posteriorly bent as in *P. schansiense*, '*P.*' *simplum*, '*P.*' *linxiaense*, and *S. lagrelii*. Moreover, *Ninxiatherium* bears very weak or no enamel plications, and its teeth are not as hypsodont. Although it is not known to what degree these features may have varied, due to the existence of only a single skull of *N. longirhinus* and *N. euryrhinus*, respectively, the differences between these two species and *P. schansiense* and *S. lagrelii* are significant enough to confirm their validity as distinct taxa. In fact, these features are somewhat more similar to '*P.*' *simplum* and '*P.*' *linxiaense*, which also bear only weak secondary enamel folds and lack the highly plicated enamel of *P. schansiense*.

Sinotherium—Ringström (1923) erected *S. lagrelii* based on a left M3 from the upper Miocene of the Shanxi Province in China. Shortly after, Ringström (1924) synonymized the genera *Parelasmotherium* and *Sinotherium*, based on their similar morphology, noting though the difference in their dimensions. The present study shows that the two elasmotheriine genera exhibit some important morphological differences. For instance, in *S. lagrelii* the D4 features a very strong crista and no crochet, while the protocone and hypocone are widely connected at about 3 cm height from the base (Ringström, 1924:fig. 4, table 12). On the contrary, in *P. schansiense* the crista is very small, and the crochet is largely developed and splits into two, while the protocone and hypocone remain separated until a later wear stage and only barely connect before the tooth is completely worn. Concerning the P4, *S. lagrelii* has a strong crista, no crochet, unfused protocone and hypocone, a strongly constricted protocone, and some enamel plications in the median valley (Ringström, 1924:fig. 1, table 12). Whereas *P. schansiense* exhibits long and narrow crista and crochet, completely fused protocone and hypocone that do not exhibit any constriction, while not exhibiting enamel plication as seen in *S. lagrelii*, as shown by the µCT analysis (Fig. 2A3–4). The molars in both *S. lagrelii* and *P. schansiense*

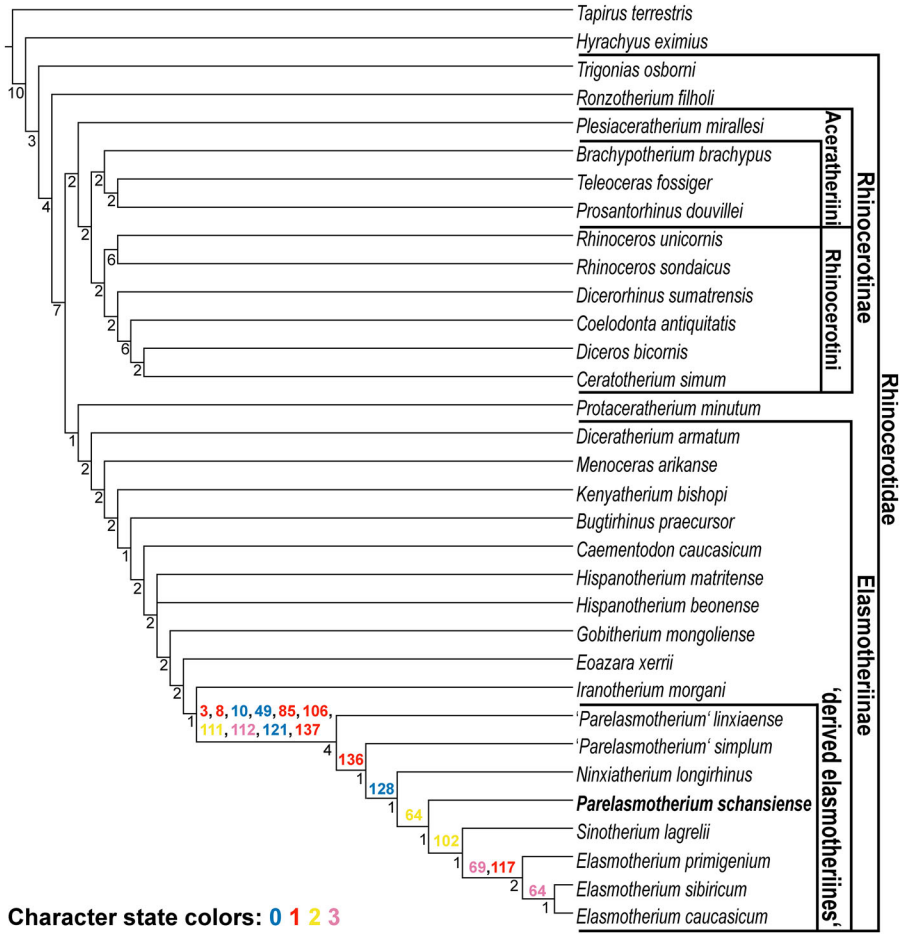

FIGURE 3. Strict consensus of the two most parsimonious trees resulting from the phylogenetic analysis. Bremer support values are reported below each branch. Synapomorphies are reported for the 'derived elasmotheriines' above the branches.

show similarly well-developed enamel plications when moderately worn (Ringström, 1924:textfigs. 87-88). However, *S. lagrelii* is much more hypsodont.

PHYLOGENETIC ANALYSIS

In order to assess the phylogenetic affinities of *Parelasmotherium* a phylogenetic analysis was performed. We modified the character-taxon matrix of Sun et al. (2021), which modified the matrix of Deng (2008) by adding *Elasmotherium primigenium*, which is based on the matrix of Antoine (2002). We also added *Eoazara xerrii* to the matrix, based on Geraads and Zouhri (2021) but removed the 32 new characters added by Lu (2013) to the matrix of Antoine (2002). '*P.*' *simplum* was scored based on published figures (Chow, 1958; Qiu and Xie, 1998) and *P. schansiense* was rescored based on the holotype (GPIT-PV-86051) studied herein. The current matrix includes 282 characters and 33 taxa (Supplementary Data 1; it is also available at MorphoBank under http://morphobank.org/permalink/?P4228). The phylogenetic analysis was performed with TNT version 1.5 (Goloboff et al., 2008). All characters were unordered. The matrix was analyzed using 'traditional search' (1000 replications), hold = 10, and random seed = 0, followed by tree bisection-reconnection. The analysis resulted in two most parsimonious trees (Figs. S1–2) with a length of 1101 steps. A strict consensus tree and decay values (Bremer support; Supplementary Data 2) were obtained using the implemented functions in TNT. Consistency (CI) and Retention indices (RI) were calculated for the whole tree (CI = 0.351 and RI = 0.543) using the script available in TNT.

DISCUSSION

Parelasmotherium schansiense has been known for almost a century (Killgus, 1923) but its exact taxonomic and phylogenetic affinities and its relationship to the other elasmotheriines of Eurasia have been debated and remain ambiguous (e.g., Deng, 2001, 2007, 2008; Antoine, 2002). The comparison to the other elasmotheriines from the upper Miocene of China showed that *P. schansiense* is a valid taxon that can be distinguished from all other species. It also showed that '*P.*' *simplum* and '*P.*' *linxiaense* exhibit important morphological differences to *P. schansiense*, such as the lack of any prominent enamel plications, implying a more derived evolutionary stage for the latter species, as suggested by the phylogenetic analysis (Fig. 3). The former two species also seem to differ from each other, as shown by the very small crista in '*P.*' *simplum*, in contrast to the largely developed crista in '*P.*' *linxiaense* and other 'derived elasmotheriines,' as suggested by the phylogenetic analysis (Fig. 3), which separates them and places both species in a more basal position than *Ninxiatherium*. Therefore, implying that *Parelasmotherium*, as it stands now, is paraphyletic and that both '*P.*' *simplum* and '*P.*' *linxiaense* should not be included in the same genus as *P. schansiense*. Thus, it might be more appropriate to refer to these two species as '*Parelasmotherium*' until these issues have been resolved.

Unfortunately, because no skulls of '*P.*' *simplum* and *P. schansiense* have been reported so far (Killgus, 1923; Chow, 1958; Qiu and Xie, 1998), important morphological features such as the morphology, number, and position of the horn boss (es) are unknown, thus making the phylogenetic position of these species more uncertain. Furthermore, the species assigned to *Parelasmotherium* and *Ninxiatherium* are represented by very few or even a single specimen. Therefore, their intraspecific variability cannot be assessed, thus complicating their comparison even further. Until additional material of these taxa becomes available, a careful and detailed description and comparison of the already known material is the only way to enhance our understanding of their relationships. Concerning *P. schansiense*, the very hypsodont teeth bearing a large crista, and rich enamel plications in the molars suggest a position among the 'derived elasmotheriines', as a sister to the clade including *Sinotherium* and *Elasmotherium*. This position is also supported by our phylogenetic analysis (Fig. 3), which might also point to an early Baodean age (Qiu et al., 2013) for Kutschwan. Furthermore, the analysis showed that the clade (marked in Fig. 3) sometimes referred to as 'derived elasmotheriines' (Deng, 2008; Deng et al., 2013) is a well-supported group (Bremer support = 4), defined by 10 synapomorphies (characters 3, 8, 10, 49, 85, 106, 111, 112, 121, 137).

CONCLUSION

Herein the holotype of the huge elasmotheriine rhinocerotid *Parelasmotherium schansiense* from the upper Miocene of Kutschwan (Shanxi, China) was re-evaluated to answer questions about its taxonomy and phylogenetic relationships. CT-scans of the specimen revealed the previously unknown morphology of the unerupted P4 and unworn M2. Comparisons with the other late Miocene elasmotheriines from China and a phylogenetic analysis showed that the genus *Parelasmotherium* is paraphyletic and therefore '*Parelasmotherium*' *simplum* and '*Parelasmotherium*' *linxiaense* should not be included in the same genus as *P. schansiense*. Furthermore, the phylogenetic analysis placed *P. schansiense* within the 'derived elasmotheriines' as a sister to the clade which includes *Sinotherium* and *Elasmotherium*.

ACKNOWLEDGMENTS

We acknowledge the support of the Centre of Visualisation, Digitisation and Replication at the Eberhard Karls Universität in Tübingen for instrument use, scientific and technical assistance and A. Tröscher (SHEP) for µCT-scanning the specimens. We thank I. Werneburg (SHEP) for the curation of the material housed in the GPIT. We would like to thank U. Göhlich (NHMW) for providing access to the collections of Maragheh. This research received support from the SYNTHESYS+ project http://www.synthesys.info/ which is financed by European Community Research Infrastructure Action under the H2020 Integrating Activities Programme, Project number 823827 (AT-TAF-TA3-9). We would like to thank the Handling Editor F. Bibi, the Technical Editor J. Harris, as well as P.-O. Antoine, and an anonymous reviewer for their helpful comments that greatly improved this work.

ORCID

Panagiotis Kampouridis http://orcid.org/0000-0002-1812-4664
Josephina Hartung http://orcid.org/0000-0002-2084-0328
Gabriel S. Ferreira http://orcid.org/0000-0003-1554-8346

LITERATURE

Andersson, J. G. 1923. Essays on the Cenozoic of northern China. Memoirs of the Geological Survey of China, Ser. A 3:1–152.

Antoine, P.-O. 2002. Phylogénie et évolution des Elasmotheriina (Mammalia, Rhinocerotidae). Mémoires du Muséum National d'Histoire Naturelle 188:1–359.

Antoine, P.-O., F. Alférez, and C. Iñigo. 2002. A new elasmotheriine (Mammalia, Rhinocerotidae) from the Early Miocene of Spain. Comptes Rendus Palevol 1:19–26.

Chen, G. F. 1977. A new genus of Iranotheriinae of Ningxia. Vertebrata PalAsiatica 15:143–147.

Chow, M. 1958. New elasmotherine rhinoceros from Shansi. Vertebrata PalAsiatica 2:131–142.

Deng, T. 2001. New remains of *Parelasmotherium* from the late Miocene in Dongxiang Gansu China. Vertebrata PalAsiatica 39:306–311.

Deng, T. 2005. New discovery of *Iranotherium morgani* (Perissodactyla, Rhinocerotidae) from the late Miocene of the Linxia Basin in Gansu, China, and its sexual dimorphism. Journal of Vertebrate Paleontology 25:442–450.

Deng, T. 2007. Skull of *Parelasmotherium* (Perissodactyla, Rhinocerotidae) from the upper miocene in the Linxia Basin (Gansu, China). Journal of Vertebrate Paleontology 27:467–475.

Deng, T. 2008. A new elasmothere (Perissodactyla, Rhinocerotidae) from the late Miocene of the Linxia Basin in Gansu, China. Geobios 41:719–728.

Deng, T., S. Wang, and S. Hou. 2013. A bizarre tandem-horned elasmothere rhino from the Late Miocene of northwestern China and origin of the true elasmothere. Chinese Science Bulletin 58:1811–1817.

Dollo, L. 1885. Rhinocéros vivants et fossiles. Revue de Questions Scientifiques 17:293–299.

Fortelius, M., and K. Heissig. 1989. The phylogenetic relationships of the Elasmotherini. Mitteilungen Der Bayerischen Staatssammlung Für Paläontologie Und Historische Geologie 29:227–233.

Geraads, D., and S. Zouhri. 2021. A new late Miocene elasmotheriine rhinoceros from Morocco. Acta Palaeontologica Polonica 66.

Geraads, D., M. McCrossin, and B. Benefit. 2012. A new rhinoceros, *Victoriaceros kenyensis* gen. et sp. nov., and other Perissodactyla from the Middle Miocene of Maboko, Kenya. Journal of Mammalian Evolution 19:57–75.

Geraads, D., T. Lehmann, D. J. Peppe, and K. P. McNulty. 2016. New Rhinocerotidae from the Kisingiri localities (lower Miocene of western Kenya). Journal of Vertebrate Paleontology 36:e1103247.

Goloboff, P. A., J. S. Farris, and K. C. Nixon. 2008. TNT, a free program for phylogenetic analysis. Cladistics 34:407–437.

Gray, J. E. 1821. On the natural arrangemenet of vertebrose animals. London Medical Repository 15:297–310.

Guérin, C. 1980. Les rhinocéros (Mammalia, Perissodactyla) du Miocène terminal au Pleistocène supérieur en Europe occidentale: comparaison avec les espèces actuelles. Département des sciences de la terre, Université Claude-Bernard Lyon 1, Villeurbanne, 3 pp.

Killgus, H. 1922. Die Unterpliocaenen Chinesischen Säugetierreste der Tafelschen Sammlung zu Tübingen. Ph.D. Dissertation, Eberhard-Karls University of Tübingen, Tübingen, Germany, 87 pp.

Killgus, H. 1923. Unterpliozäne Säuger aus China. Paläontologische Zeitschrift 5:251–257.

Kosintsev, P., K. J. Mitchell, T. Devièse, J. van der Plicht, M. Kuitems, E. Petrova, A. Tikhonov, T. Higham, D. Comeskey, C. Turney, A. Cooper, T. van Kolfschoten, A. J. Stuart, and A. M. Lister. 2019. Evolution and extinction of the giant rhinoceros *Elasmotherium sibiricum* sheds light on late Quaternary megafaunal extinctions. Nature Ecology & Evolution 3:31–38.

Linnaeus, C. 1758. Systema Naturae. Laurentii Salvii, Stockholm, pp.

Liu, S., M. V. Westbury, N. Dussex, K. J. Mitchell, M.-H. S. Sinding, P. D. Heintzman, D. A. Duchêne, J. D. Kapp, J. von Seth, H. Heiniger, F. Sánchez-Barreiro, A. Margaryan, R. André-Olsen, B. De Cahsan, G. Meng, C. Yang, L. Chen, T. van der Valk, Y. Moodley, K. Rookmaaker, M. W. Bruford, O. Ryder, C. Steiner, L. G. R. Bruins-van Sonsbeek, S. Vartanyan, C. Guo, A. Cooper, P. Kosintsev, I. Kirillova, A. M. Lister, T. Marques-Bonet, S. Gopalakrishnan, R. R. Dunn, E. D. Lorenzen, B. Shapiro, G. Zhang, P.-O. Antoine, L. Dalén, and M. T. P. Gilbert. 2021. Ancient and modern genomes unravel the evolutionary history of the rhinoceros family. Cell S0092867421008916.

Lu, X. 2013. A juvenile skull of *Acerorhinus yuanmouensis* (Mammalia: Rhinocerotidae) from the Late Miocene hominoid fauna of the Yuanmou Basin (Yunnan, China). Geobios 46:539–548.

Mecquenem, R. de. 1908. Le lac D'ourmiah. Annales de Géographie 17:128–144.

Pandolfi, L. 2016. *Persiatherium rodleri*, gen. et sp. nov. (Mammalia, Rhinocerotidae) from the upper Miocene of Maragheh (northwestern iran). Journal of Vertebrate Paleontology 36:e1040118.

Qiu, Z., and J. Xie. 1998. Notes on *Parelasmotherium* and *Hipparion* fossils from Wangji, Dongxiang, Gansu. Vertebrata PalAsiatica 36:13–23.

Qiu, Z. X., Z. D. Qiu, T. Deng, C. K. Li, Z. Q. Zhang, B. Y. Wang, and X. Wang. 2013. Neogene land mammal stages/ages of China; pp. 29–90 in X. Wang, L. J. Flynn, and M. Fortelius (eds.), Fossil Mammals of Asia. Columbia University Press, New York.

Ringström, T. 1923. *Sinotherium lagrelii*. Ringström. A new fossil rhinocerotid from Shansi, China. Bulletin of the Geological Survey of China 5:91–93.

Ringström, T. 1924. Nashörner der Hipparion-Fauna Nord-Chinas. Palaeontologia Sinica 1:1–156.

Schvyreva, A. K. 2015. On the importance of the representatives of the genus *Elasmotherium* (Rhinocerotidae, Mammalia) in the biochronology of the Pleistocene of Eastern Europe. Quaternary International 379:128–134.

Sun, D.-H., T. Deng, and Q. Jiangzuo. 2021. The most primitive *Elasmotherium* (Perissodactyla, Rhinocerotidae) from the Late Miocene of northern China. Historical Biology 1–11.

Tafel, A. 1914. Meine Tibetreise. Eine Studienfahrt Durch Das Nordwestliche China Und Durch Die Innere Mongolei in Das Östliche Tibet. Union Deutsche Verlagsgesellschaft, Stuttgart, 352 pp.

Submitted January 28, 2022; revisions received April 28, 2022;
accepted May 10, 2022.
Handling Editor: F. Bibi.